Synthesis and CO Gas-Sensing Properties of CuO and Spinel Ferrite Nanocomposite Thin Films

L. Presmanes*, A. Chapelle, F. Oudrhiri-Hassani, A. Barnabé, and Ph. Tailhades

Institut Carnot CIRIMAT, UPS-INPT-CNRS 5085,
Université Paul Sabatier 118 route de Narbonne 31 062 Toulouse Cedex 9, France

A nanocomposite thin film composed of tenorite (CuO) and spinel ferrite ($Cu_xFe_{3-x}O_4$) has been prepared by radio-frequency sputtering method followed by a post-deposition thermal annealing. The nanostructure was examined by grazing X-ray diffraction, atomic force microscopy and scanning electron microscopy. CuO-$Cu_xFe_{3-x}O_4$ nanocomposite layer was deposited on the top of screen-printed gold electrodes onto SiO_2(200 nm)/Si substrate. It was found that this material contains *p–n* nano-heterojunctions, was sensitive to 500 ppm carbon monoxide at the operational temperature of 400 °C and exhibited a large response of 90%.

Keywords: Nanocomposites, Thin Films, Sputtering, CuO, Spinel Ferrite, Gas Sensors, Carbon Monoxide.

1. INTRODUCTION

Nanocomposites have received great attention due to their unique mechanical, optical, electrical, thermal or magnetic properties.[1–3] In this large family, oxide/oxide nanocomposites have been reported for many applications such as photocatalysis and photoelectric transition,[4] microelectronics,[5] solar cells,[6] and electroluminescence.[6]

Nanocomposites based on semiconductor metal oxides are also of great interest for creation of selective gas sensors[7, 8] and have been employed for the detection of carbon monoxide (CO). CO sensors are essential to the control of the emissions from combustion processes. In addition, the toxic nature of CO makes the detection of this gas for household and environmental applications necessary. The detection of CO is therefore an extremely important research area. Recently, composites made of *p*-type copper oxide and various *n*-type metal oxides such as CuO/SnO₂ and CuO/ZnO have been studied as gas sensors to detect H_2S, H_2 and CO gas.[9–11]

Several techniques such as ion implantation,[12] sputtering,[13–15] and electrodeposition[16] have been used for the preparation of nanocomposites films. In the form of thin films, these materials allow mass production of devices at low cost with high control and repeatability. Moreover, due to their high intrinsic surface-to-volume ratio, nanostructured thin films exhibit high capabilities for miniaturization. Among all the available processes, radio-frequency (RF) sputtering is particularly suitable for the preparation of nanocomposite films with a good homogeneity. In this context, it can be advantageous to prepare sensing layers containing *p–n* heterojunctions at the nanometric scales by RF sputtering process, and to use this process compatibility with the microelectronic technology, and with elaboration of micro-sensors.

We have already shown that RF sputtering can lead to the preparation of various nanocomposite thin films.[17–19] Additionally, we have recently highlighted the CO₂ sensing properties at low temperature (250 °C) for nanocomposite thin layers made of *p*-type CuO and *n*-type $Cu_xFe_{3-x}O_4$.[20] In this paper, we report the synthesis of a $CuO/Cu_xFe_{3-x}O_4$ thin film elaborated by RF sputtering followed by a post-deposition annealing—resulting in nanosized and well dispersed particles in the structure. We then present carbon monoxide sensing properties of this thin film at different temperatures.

2. EXPERIMENTAL DETAILS

Thin films were deposited with an Alcatel A450 apparatus using a home-made sintered ceramic target of pure $CuFeO_2$ with a relative density of 70%. The RF power was set at 4 W/cm² and the pressure inside the deposition

*Corresponding author; E-mail: presmane@chimie.ups-tlse.fr

chamber was lower than 5×10^{-6} mbar prior to deposition. During the elaboration of the films, the argon pressure and the target-to-substrate distance were adjusted to 2 Pa and 8 cm, respectively. 300 nm thick films were deposited on glass substrate for structural and microstructural characterizations. The film thickness was fixed to a value of 50 nm on test device for the determination of CO sensing properties.

Structural phase analyses such as Grazing Incidence X-Ray Diffraction (GXRD) (grazing angle $\alpha = 1°$) were carried out with a Siemens D5000 diffractometer using the copper $K\alpha$ radiation. The morphology of the thin film was determined by Scanning Electron Microscopy using a Field Emission Gun (FEG-SEM) Jeol JSM 6400 and a Veeco Dimension 3000 Atomic Force Microscope (AFM) equipped with a super sharp TESP-SS Nanoworld© tip (nominal resonace frequency 320 kHz, nominal radius curvature 2 nm).

Our simplified test device consists of a silicon wafer substrate electrically insulated with a 1 μm thick SiO_2 blanket-layer. Two gold interdigitated electrodes were screen-printed onto the surface of the silicon dioxide layer. The drying and densification of the gold paste was made by thermal annealing at 700 °C. The sensing nanocomposite layer was then deposited on the top of the electrode by RF-sputtering with the electrical contacts at each side of the electrodes left uncovered.

The electrical response of the sensing layer was investigated by registering the variations in impedance with a RCL-meter (FLUKE PM6306) as a function of temperature and time. The test device was placed in a furnace operating under controlled atmosphere with the temperature range of 20–480 °C. The total gas flow was fixed at 100 cm^3/min. Two bottles equipped with mass flow regulators were used to set the CO concentrations at 500 ppm. Therefore, a low frequency was used to avoid the relaxation phenomenon and to acquire signals due to the spatial-charge phenomenon. An arbitrary value of 700 Hz was chosen.

The response R is defined by Eq. (1) as follows:

$$R(\%) = 100 \times ((Z_{CO} - Z_{air})/Z_{air}) \tag{1}$$

where Z_{air} and Z_{CO} are the electrical impedances of the sensor measured in air and in CO respectively. Electrical responses were recorded at different temperatures, with alternating air and CO pulses.

3. RESULTS AND DISCUSSION

3.1. Synthesis and Characterization

The deposition of the film by RF sputtering constitutes the first step of the preparation process. In the Figure 1(a) the GXRD pattern of the as-deposited thin film shows a broad peak located at $2\theta = 35.5$ deg, i.e., with $d_{hkl} \approx 2.5$ Å which
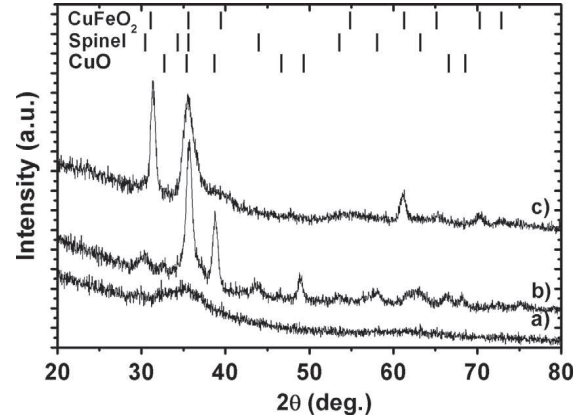

Fig. 1. Grazing angle X ray diffraction patterns of the deposited film on glass substrate from a $CuFeO_2$ target, (a) As-deposited film. (b) After annealing in air at 450 °C for 24 hours. (c) After annealing film under vacuum at 450 °C for 15 hours. Thickness = 300 nm. $P = 2$ Pa, $d = 8$ cm.

could be attributed to $CuFeO_2$ ($d_{012} = 2.51$ Å). However, delafossite phase cannot be unambiguously identified using GXRD, in the as-deposited film, due to the nano-crystallinity of the material. Apart from the preparation process, an additional thermal annealing under vacuum at 450 °C was performed in order to increase the crystallite size of the phase and to clearly reveal the diffraction peak related to delafossite phase (Fig. 1(c)). By using high deposition pressure and large target to substrate distance, the oxidation state of copper which is +I in the delafossite target has been then preserved in the deposited layer. Moreover no metallic copper is detected contrary to others films deposited at low pressure and low target-to-substrate distance.[17, 20] Indeed, with a high deposition pressure and large target to substrate distance during the sputtering process, the particles ejected from the target undergo many collisions during the transfer to the substrate, leading to lower energies and thus less oxygen ejected in the growing layer.

The second step in the preparation of CuO-$Cu_xFe_{3-x}O_4$ composite consists of heat treatment of the as-deposited film in air at 450 °C. According to the phase diagram,[21] this treatment leads to the decomposition of nano-crystallized delafossite $CuFeO_2$ into tenorite (CuO) and cuprospinel ($Cu_xFe_{3-x}O_4$ with x close to 1) phases in line with the GXRD pattern (Fig. 1(b)).

This two steps process allowed us to obtain nanocomposites thin film containing p-type CuO[22, 23] and n-type $Cu_xFe_{3-x}O_4$[24, 25] semiconducting phases well dispersed. The average grain size for the thin film surface, determined from an AFM image was around 50–60 nm (Fig. 2(a)) and confirmed by a SEM-FEG image (Fig. 2(b)). By profile fitting in XRD pattern, we obtain a crystallite size of 50 nm for CuO particles by using Scherrer equation corrected by instrumental contribution. The nanometric p–n heterojunctions easily obtained from this process is of great interest for the field of sensing layers for semiconductor gas sensors.
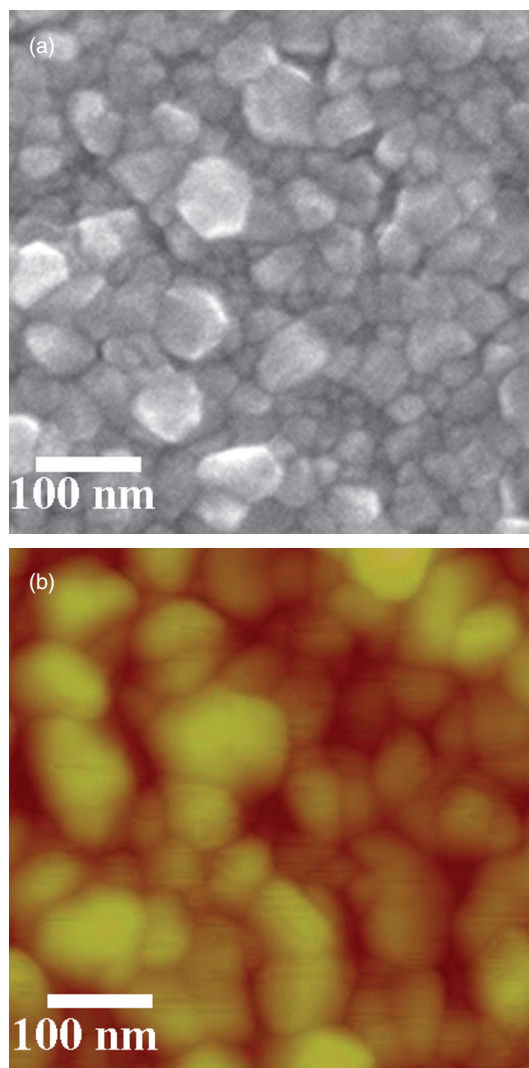
Fig. 2. SEM-FEG (a) and AFM (b) images after annealing in air at 450 °C for 12 hours. Thickness = 300 nm. $P = 2$ Pa, $d = 8$ cm.

3.2. CO Gas Sensing Properties

The CO gas sensing experiments of the simplified test device covered with the nanocomposite layer were performed at different temperatures in order to find out the optimum operating temperature. The response of our sensing layer to 500 ppm concentration of CO and in a temperature range of 200–450 °C is illustrated in Figure 3. The operating temperature has an increased influence on the response to CO gas. A typical temperature dependant behavior showing a maximum response has been widely reported in the literature for a variety of semi-conducting materials. This phenomenon is generally explained by the thermally activated adsorption and desorption of oxygen and CO at the surface of the sensing layer. Other models take in account the width of a depletion layer between the semi-conducting grains which is temperature dependent. The temperature that gives the optimal response depends on the composition and the doping of the oxide used as
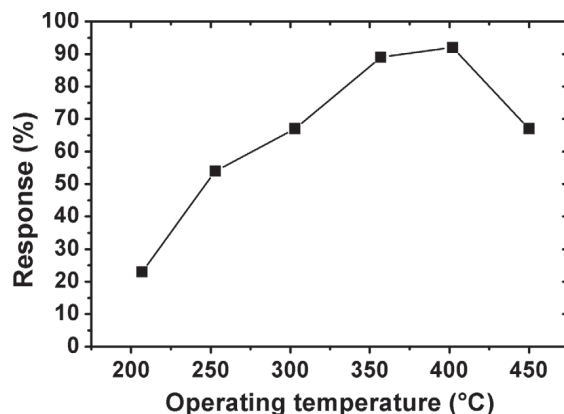

Fig. 3. Response as a function of operating temperature of the CuO-$Cu_xFe_{3-x}O_4$ layer deposited on screen-printed gold electrodes under CO atmosphere. $P = 2$ Pa, $d = 8$ cm, $f = 700$ Hz, flow = 100 sccm, [CO] = 500 ppm, $e = 50$ nm.

sensitive layer. For a given material, the grain size and the grain boundaries have also a great influence on the optimal temperature. In our case, the evolution of the response of the layer shows that this maximum is located around 400 °C.

Figure 4 shows the impedance transient of the nanocomposite layer recorded at the optimum temperature of 400 °C with alternating air and air+CO (500 ppm) pulses. The positive response observed (i.e., $Z_{CO} > Z_{air}$) is representative of the interaction of CO which is a reducing gas (electron donor) with a p-type semiconductor, by decreasing the number of holes. This suggests that the role of p-type CuO in the nanocomposite is predominant. We have seen in previous paper[20] that the interaction of CuO-$Cu_xFe_{3-x}O_4$ nanocomposite with an oxidizing gas such as CO_2 led to a negative response and then also behaved like in the presence of a p-type semiconductor. The best response was found to be approximately 90% at 400 °C, which corresponds to a Z_{CO}/Z_{air} ratio of 1.9.

Response and recovery times, which are defined as the time to reach 90% of the final signal level, are important characteristics of a gas sensor. As depicted in Figure 4,
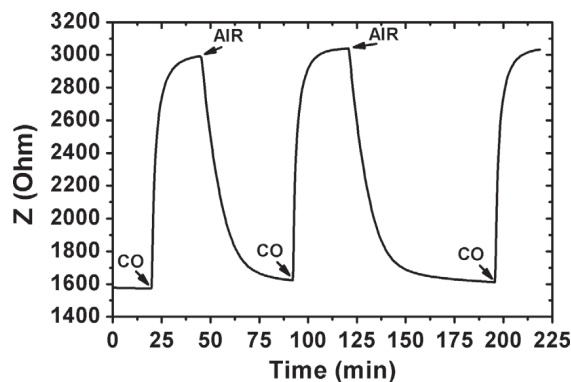

Fig. 4. Impedance transient of CuO-$Cu_xFe_{3-x}O_4$ thin film deposited on screen printed gold electrodes. $P = 2$ Pa, $d = 8$ cm, $T = 400$ °C, $f = 700$ Hz, flow = 100 sccm, [CO] = 500 ppm, $e = 50$ nm.

the sensing layer exhibits response and recovery times of 21 min and 8 min respectively, as well as a good reversibility.

4. CONCLUSIONS

Based on the results and discussion, we can conclude that the nanocomposites $CuO-Cu_xFe_{3-x}O_4$ can be easily prepared by a two step process. A $CuFeO_2$ phase was first deposited and then annealed in air at 450 °C to lead to the decomposition of the phase. In comparison with the elaboration of multi-layers composites artificially stacked, the interest of our method is that these nanocomposites have been obtained directly, after a simple thermal annealing, by using oxidation and decomposition phenomena expected from Fe-Cu-O phase diagram. Moreover, we can expect a good quality interface between the two n-type and p-type phases that are self-mixed at a nanometric scale. The particles sizes of the nanocomposites were obtained in the range of 50–60 nm. The $CuO-Cu_xFe_{3-x}O_4$ sensing layer showed a response of 90% to 500 ppm CO at 400 °C, with a good reversibility.

References and Notes

1. A. Z. Sadek, W. Wlodarski, K. Shin, R. B. Kaner, and K. Kalantar-Zadeh, *Nanotechnology* 17, 4488 (**2006**).
2. L. Al-Mashat, K. Shin, K. Kalantar-Zadeh, J. D. Plessis, S. H. Han, R. W. Kojima, R. B. Kaner, D. Li, X. L. Gou, S. J. Ippolito, and W. Wlodarski, *J. Phys. Chem. C* 114, 16168 (**2010**).
3. K. Galatsis, Y. X. Li, W. Wlodarski, and K. Kalantar-zadeh, *Sens. Actuators, B-Chemical* 77, 478 (**2001**).
4. X. Su, J. Zhao, Y. Li, Y. Zhu, X. Ma, F. Sun, and Z. Wang, *Colloids Surf., A: Physicochem. Eng. Aspects* 349, 151 (**2009**).
5. R. K. Goyal, A. N. Tiwari, U. P. Mulik, and Y. S. Negi, *Compos. Sci. Technol.* 67, 1802 (**2007**).
6. U. Pal, J. García-Serrano, G. Casarrubias-Segura, N. Koshizaki, T. Sasaki, and S. Terahuchi, *Sol. Energy Mater. Sol. Cells* 81, 339 (**2004**).
7. Y. X. Li, K. Galatsis, W. Wlodarski, M. Passacantando, S. Santucci, P. Siciliano, and M. Catalano, *Sens. Actuators, B-Chemical* 77, 27 (**2001**).
8. M. B. Rahmani, S. H. Keshmiri, M. Shafiei, K. Latham, W. Wlodarski, J. du Plessis, and K. Kalantar-Zadeh, *Sensors Lett.* 7, 621 (**2009**).
9. L. A. Patil and D. R. Patil, *Sens. Actuators, B-Chemical* 120, 316 (**2006**).
10. Y. Zeng, T. Zhang, H. Yang, L. Qiao, Q. Qi, F. Cao, Y. Zhang, and R. Wang, *Appl. Surf. Sci.* 255, 4045 (**2009**).
11. S. Aygun and D. Cann, *J. Phys. Chem. B* 109, 7878 (**2005**).
12. U. Pal, A. Bautista-Hernandez, L. Ridriguez-Fernandez, and J. C. Cheang-Wong, *J. Non-Cryst. Solids* 275, 65 (**2000**).
13. M. Pal, T. Sasaki, and N. Koshizaki, *Scr. Mater.* 44, 1817 (**2001**).
14. D. H. Trinh, T. Kubart, T. Nyberg, M. Ottosson, L. Hultman, and H. Högberg, *Thin Solid Films* 23, 8352 (**2008**).
15. A. Romanyuk, R. Steiner, L. Marot, V. Spassov, and P. Oelhafen, *Thin Solid Films* 516, 8513 (**2008**).
16. T. Yoshino, S. Takanesawa, T. Ohmori, and H. Masuda, *Jpn. J. Appl. Phys.* 35, L1512 (**1996**).
17. E. Mugnier, A. Barnabé, L. Presmanes, and Ph. Tailhades, *Thin Solid Films* 516, 1453 (**2008**).
18. B. Mauvernay, L. Presmanes, S. Capdeville, V. G. de Resende, E. De Grave, C. Bonningue, and Ph. Tailhades, *Thin Solid Films* 515, 6532 (**2007**).
19. B. Mauvernay, L. Presmanes, C. Bonningue, and Ph. Tailhades, *J. Magn. Magn. Mater.* 320, 58 (**2008**).
20. A. Chapelle, F. Oudrhiri-Hassani, L. Presmanes, A. Barnabé, and Ph. Tailhades, *Appl. Surf. Sci.* 256, 4715 (**2010**).
21. A. G. Zalazinskii, V. F. Balakirev, and G. I. Chufarov, *Zh. Fiz. Khim.* 43, 1636 (**1969**).
22. M. Muhibbullah, M. O. Hakim, and M. G. M. Choudhury, *Thin Solid Films* 423, 103 (**2003**).
23. Y. K. Jeong and G. M. Choi, *J. Phys. Chem. Solids* 57, 81 (**1996**).
24. S. Tao, F. Gao, X. Liu, and O. T. Sorensen, *Mater. Sci. Eng., B* 77, 172 (**2000**).
25. A. N. Patil, R. P. Mahajan, K. K. Patankar, A. K. Ghatage, V. L. Mathe, and S. A. Patil, *Indian J. Pure Appl. Phys.* 38, 651 (**2000**).